Human Molecular Genetics, 2007, Vol. 16, No. 7 **848–864**
doi:10.1093/hmg/ddm030
Advance Access published on February 22, 2007

CHIP and HSPs interact with β-APP in a proteasome-dependent manner and influence Aβ metabolism

Pravir Kumar[1], Rashmi K. Ambasta[2], Vimal Veereshwarayya[1], Kenneth M. Rosen[1], Ken S. Kosik[3], Hamid Band[4], Ruben Mestril[5], Cam Patterson[6] and Henry W. Querfurth[1,*]

[1]Department of Neurology, Caritas St Elizabeth's Medical Center, Tufts University School of Medicine, 736 Cambridge Street, Boston, MA 02135, USA, [2]Boston Biomedical Research Institute, Watertown, MA 02472, USA, [3]Department of Molecular Cellular and Developmental Biology, UCSB, Santa Barbara, CA 93106, USA, [4]ENH Research Institute, 1001 University Place, Evanston, IL 60201, USA, [5]The Cardiovascular Institute, Loyola University Medical Center, IL 60153, USA and [6]Carolina Cardiovascular Biology Center, University of North Carolina, Chapel Hill, NC 27599, USA

Received February 9, 2007; Revised and Accepted February 12, 2007

The C-terminus Hsp70 interacting protein (CHIP) has dual function as both co-chaperone and ubiquitin ligase. CHIP is increasingly implicated in the biology of polyglutamine expansion disorders, Parkinson's disease and tau protein in Alzheimer's disease. We investigated the involvement of CHIP in the metabolism of the β-amyloid precursor protein and its derivative β-amyloid (Aβ). Using immunoprecipitation, fluorescence localization and crosslinking methods, endogenous CHIP and βAPP interact in brain and cultured skeletal myotubes as well as when they are expressed in stable HEK cell lines. Their interaction is confined to Golgi and ER compartments. In the presence of the proteasome inhibitor with MG132, endogenous and expressed βAPP levels are significantly increased and accordingly, the interaction with CHIP enhanced. Concurrently, levels of Hsp70 were most consistently induced by proteasome inhibition among the various heat shock proteins (HSPs) tested. Thus, complexes of CHIP, Hsp70 and holo-βAPP (as well as C-terminal fragments) were stabilized by the action of MG132. Moreover, CHIP itself is shown to both increase cellular holo-βAPP levels and protect it from oxidative stress and degradation. Interestingly, CHIP also promotes the association of ubiquitin with βAPP, implying that a smaller pool of βAPP is destined for proteasomal processing. In neuronal cultures, CHIP and Hsp70/90 expression reduce steady-state cellular Aβ levels and hasten its degradation in pulse-chase experiments. The functional significance of CHIP and HSP interactions, especially with Hsp70, was tested using siRNA and in neuronal cells where protection from Aβ-induced toxicity is shown. We conclude that CHIP, as a bimolecular switch, interacts with HSP to stabilize normal holo-βAPP on the one hand while also assisting in the ubiquitination of a subpopulation of βAPP molecules that are destined for proteasome degradation. CHIP also hastens the clearance of Aβ in a manner consistent with its known neuroprotective properties.

INTRODUCTION

A large body of evidence supports the hypothesis that the accumulation of intracellular Aβ42 is an early event in the pathogenic cascade of Alzheimer's disease, resulting in neuronal dysfunction, synaptic/neuronal loss and clinical dementia (1–9). Several recent studies have suggested that certain molecular chaperones, heat shock proteins (HSPs) Hsp70 and Hsp90 and co-chaperones, e.g. C-terminus of Hsp70 interacting protein (CHIP), assume important roles in maintaining protein homeostasis in a crowded cytoplasmic milieu. These act to lessen the toxicity of misfolded and aggregated proteins in polyglutamine expansion disorders and other neurodegenerative conditions (10–13). Previously, we have reported that Hsp70 participates in the neuroprotective response to the expression and accumulation of intracellular β-amyloid

*To whom correspondence should be addressed at: Tel: +1 6177892685; Fax: +1 6177895177; E-mail: henry.querfurth@tufts.edu

(14,15). To better understand the roles of molecular chaperones in the biochemical events associated with β-amyloid-induced neurodegeneration, we have examined the function and interactions of the Hsp70 client protein, CHIP.

CHIP is a ubiquitously expressed cytoplasmic protein that is structurally conserved across multiple species and is highly expressed in brain, heart and muscles (16). The N-terminal region of CHIP has three tetratricopeptide repeat domains, which are responsible for protein–protein interactions with HSPs 70/90 and other molecular chaperones including Hip, Hop, Cyclophilin 40, FKBP52 and Bag1 phosphatase 5 (17–20). The CHIP C-terminus contains a U-box, or RING finger-like domain, which is the site of its ubiquitin (UBQ) E3 ligase activity (21). Owing to these dual capacities, CHIP acts as a molecular triage center (22) linking the chaperones to the UBQ proteasome system. CHIP is a critical switch that controls protein fate by orchestrating attempts at re-folding versus degrading misfolded proteins (23,24).

Recent studies have implicated CHIP and its UBQ ligase activity in interactions with proteins harboring expanded polyglutamine tracts by targeting them for degradation in the proteasomal system (13,25). Thus, CHIP is co-immunoprecipitated with huntingtin and ataxin-3, whereas overexpression of CHIP leads to increased ubiquitination and degradation of both mutant polyQ-modified proteins (25). A wider role for CHIP in other neurodegenerative conditions has been suggested from studies implicating it in familial Parkinson's disease, where it has been found to assist in the dissociation of Hsp70 from a complex with Parkin and PAEL-R, facilitating Parkin-mediated PAEL-R ubiquitination (26). CHIP appears to mediate, at least in part, the degradation of α-synuclein by triaging between the proteasomal and lysosomal pathways (27). CHIP also targets the immature CFTR protein for proteasomal degradation (28,29). Recently, a possible role for CHIP in the cellular response to tau-protein stress has been uncovered, where it was shown to polyubiquitinate phosphorylated 4-repeat-tau, attenuate tau aggregation and enhance cell survival (30–32).

In addition to these associations, CHIP induces trimerization of the transcription factor HSF1, leading to the activation of HSP genes and induction of a protective program against apoptosis and cellular stress (33,34). The multifunctional CHIP also influences Hsp70 levels by an additional mechanism that is independent of HSF1 transcriptional activation and opposite in effect (35). This showed that CHIP not only enhances Hsp70 induction during acute stress but it also mediates the turnover of Hsp70 during stress recovery. The biphasic regulation of Hsp70 highlights the existence of a competition between Hsp70 and other substrates for CHIP's ubiquitination action. CHIP appears to sense stress protein levels in its decision to terminate Hsp70 action. Thus when CHIP molecules are involved in the modification and targeting of a misfolded protein for degradation, Hsp70 levels are induced. When the substrate is eventually returned to a normal conformation or levels of its denatured form are eliminated, CHIP then functions to degrade its partner (35). In so doing, basal levels of Hsp70 are re-established.

In the present investigation, by studying the interactions between CHIP, HSPs and the β-amyloid precursor protein (βAPP), we hypothesized that CHIP may have a more universal range of substrates with respect to neurodegenerative proteins. Our investigations examined this question in both endogenous and cell culture overexpression models. We indeed find that these three proteins interact natively and that this interaction is enhanced in the presence of proteasomal inhibition. Laser scanning confocal microscopy was used to probe the subcellular regions of interaction. The colocalization results implicate the ER and Golgi compartments. Interestingly, overexpression of CHIP appears to stabilize steady-state holo-βAPP levels, in part through changes in the rate of βAPP maturation and degradation. On the other hand, CHIP also promotes the association of some βAPP with ubiquitin (UBQ), presumably in preparation for degradation. Moreover, CHIP, in complex with several HSPs, is part of a machinery that attenuates $A\beta_{42}$ peptide levels in both SH-SY5Y neuroblastoma cells and in cultures of primary cortical neurons. These results suggest that CHIP has dual roles with contrasting effects on βAPP metabolism: as co-chaperone to induce proper folding and lessen degradation of holo-APP and as probable intermediate to another E3 ligase that ubiquitinates βAPP. In addition to these, CHIP appears to hasten the degradation of β-amyloid, an undesirable βAPP metabolite. A switch-like property between these bifunctional activities is consistent with CHIP action on other substrates.

RESULTS

Identification of CHIP–APP and APP–UBQ complexes: stabilization with inhibition of the proteasome

Our previous finding of chaperone induction, specifically Hsp70, in a cell culture model of Alzheimer's disease-type cellular stress (15) led us to investigate the possibility of interaction between the Hsp70 client protein CHIP and holo-βAPP or with products of β and β/γ-secretase action on βAPP, C99 and Aβ, respectively. Since the C-terminal, cytoplasmic region of βAPP has been shown to undergo ubiquitination (36,37) and the co-chaperone/UBQ ligase CHIP, together with Hsp70 and the other molecular chaperones, functions to triage proteins destined for correct folding or UBQ-proteasome-dependent degradation, we studied the effect of proteasome inhibition, using MG132 on CHIP–APP–HSP complex formation and on the levels of the individual components. Our initial experiments utilized differentiated mouse C2C12 myotubes, an abundant source of endogenous βAPP (38). Later experiments confirmed those results in an HEK cell line that overexpresses βAPP.

In Figure 1A (top), western analysis reveals that proteasomal inhibition using MG132 leads to an increase in steady-state, endogenous βAPP levels in C2C12 myotubes and a minor change in basal CHIP. Lactacystin treatment led to the same result (not shown). We next used immunoprecipitation (IP) followed by western blot to determine whether an interaction between βAPP and CHIP could be demonstrated. IP of CHIP from myotube extracts led to the pull-down of βAPP and vice versa, an effect that was enhanced in the presence of proteasomal inhibition (Fig. 1A, middle

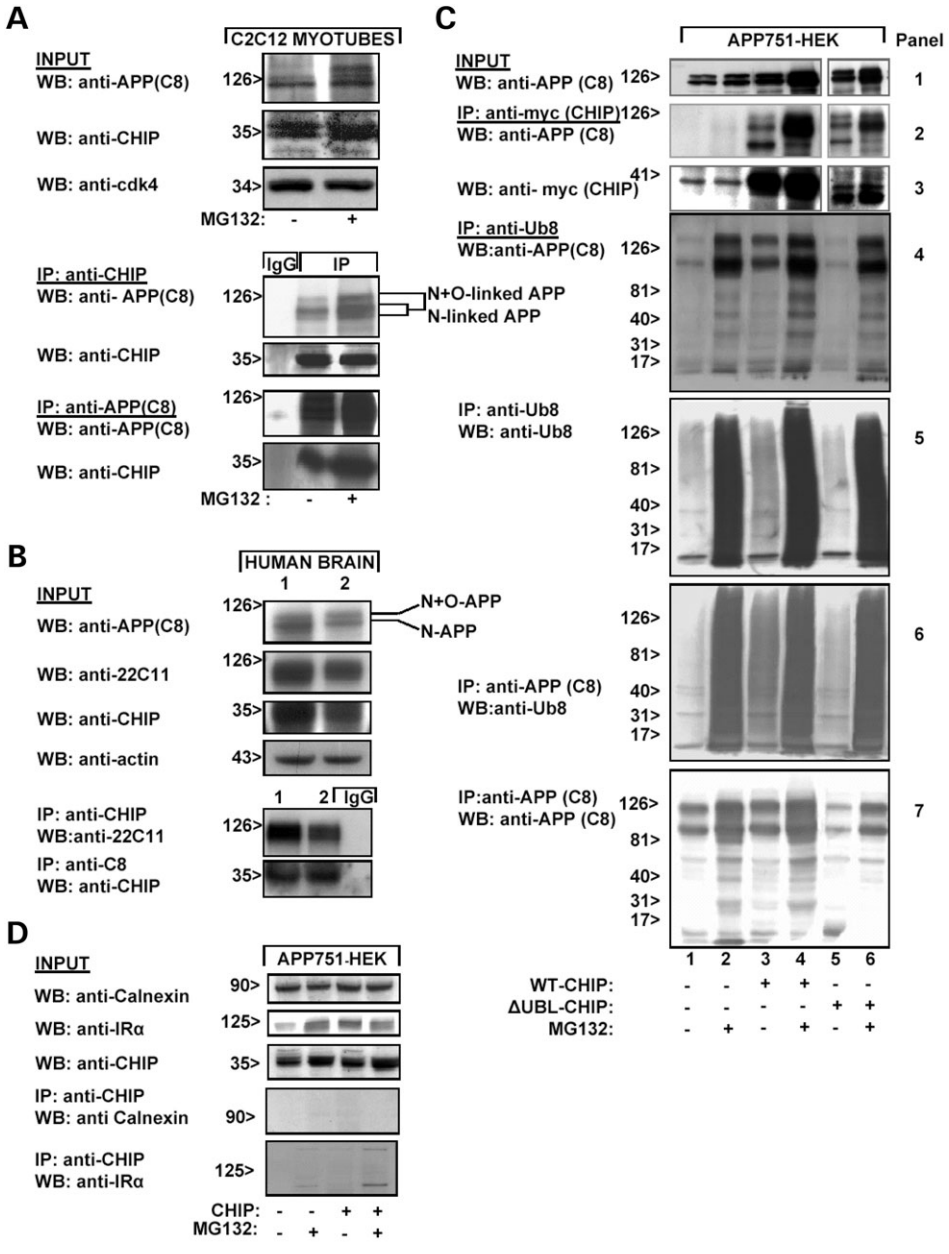

Figure 1. Interaction of holo-βAPP and CHIP in both endogenous and overexpression systems. (**A**) Upper panel: Western blot analysis for endogenous expression levels of both APP and CHIP in whole-cell lysates from C2C12 myotubes cultured in the presence (+) or absence (−) of proteasome inhibitor MG132 and fractionated on 8% polyacrylamide gel. cdk4 was used as a control for loading. IPs using either anti-CHIP (middle) or anti-βAPP (lower) followed by western blot reveal an interaction between APP and CHIP, which is enhanced in the presence of the proteasome inhibitor MG132. Non-immune IgG was used as a control for specificity. (**B**) Extracts of human brain tissue were used for western blot analysis, IP and inverse IP, as described in (A). βAPP expression was detected using both anti-C8 and anti-22C11 antibodies. CHIP expression was detected using rabbit polyclonal anti-CHIP, whereas anti-actin served as a loading control. Duplicate IPs followed by western blot with either anti-CHIP or anti-APP identify the presence of the CHIP–APP complex in human brain. (**C**) Stable APP751-HEK cells were transiently transfected with WT- or ΔUBL-CHIP in the presence or absence of MG132. Top three panels denote input and IPs using anti-myc epitope antibody (for CHIP) followed by western blot for βAPP. MG132 enhances the association of APP with both WT and the mutant ΔUBL-CHIP. Lanes 1 and 2 show a common non-specific reaction using this antibody to myc. Middle two and lower two panels: IP with anti-UBQ followed by APP western blot and inverse IP with anti-APP followed by UBQ immuno blot identify full-length APP in weak association with UBQ (lane 1). The association is greatly increased in the presence of exogenous WT (lanes 3 and 4) but not mutant CHIP (lane 5) as well as generally by inhibition of the proteasome (lanes 2, 4 and 6). Stripping and re-probing of these blots with anti-UBQ do not identify any overall alteration in ubiquitinated proteins under the different conditions. Proteasome inhibition and/or WT CHIP expression is shown to enhance APP expression in the stably transfected cell line (bottom panel) as it with endogenous level (C2C12 myotubes and SHSY5Y cells). (**D**) Control IPs using anti-CHIP do not show interaction with either calnexin or the insulin receptor (alpha) subunit.

and lower panel). This interaction appears to not be limited to muscle because we used the same methodology to identify complex formation between CHIP and APP in samples prepared from human brains (Fig. 1B). This interaction was further probed in a stably transfected HEK293 cell line expressing wild-type (WT) human APP751 (APP751-HEK). Transient transfection of these cells with myc-tagged CHIP expression constructs demonstrates again the interaction between CHIP and APP (Fig. 1C, panel 2, lane 3). We additionally found that the use of a mutant CHIP, lacking its U-box ligase domain, was still capable of interacting with APP in a proteasome sensitive manner (lane 5). Importantly, CHIP expression and proteasome inhibition each appears to raise holo-βAPP in whole-cell extracts (lanes 2–4 versus 1, see also panel 6 below).

APP751-HEK cells were used next to determine whether CHIP expression and complex formation with APP have the expected effect to promote either the association of UBQ with APP or the direct UBQ modification of βAPP. In Figure 1C, panel 4, WT CHIP expression increased the pull down of APP with anti-UBQ antibodies (lane 3 versus 1). In the presence of MG132, the level of APP-UBQ complex was also upregulated but to an even greater extent (lane 2 versus 1). The combination of CHIP and MG132 provides a slight boost relative to MG132 alone (lane 4 versus 2). Conversely, in the absence of the UBL domain, little APP (although still bound to CHIP, Fig. 1C, panel 2) is associated with UBQ (panel 4, lane 5 versus 3). The importance of the CHIP U-box domain in client substrate ubiquitination is documented in the case of CFTR protein (28) and ataxin-3 (25). Proteasome inhibition, as anticipated, floods the cells with UBQ (panel 5) and drives many UBQ reactions (e.g. panels 4, 5 and 6; lane 6). The specificity of the CHIP–APP interaction was supported by the absence of the association between CHIP and either calnexin or the α -subunit of the insulin receptor (Fig. 1D). Both control proteins are endoplasmic reticulum (ER) residents.

Functional aspects of CHIP–APP complex formation

In order to test whether APP engages with endogenous CHIP, form complexes in the stable APP751-HEK cells, we used a thiol cleavable, homobifunctional crosslinking reagent with a 12 Å spacer in cell extracts. In Figure 2A, two high molecular weight signals of ∼150 and 190 kDa were detected, which were immunoreactive to the anti-APP or anti-CHIP (brackets). Since the same signals disappear under reducing conditions, it is possible that they correspond to complexes of APP with one (maximum two) CHIP molecule plus a variable contribution from Hsp70. Next, we asked whether the APP subpopulation bound to CHIP is itself ubiquitinated. The logic follows from CHIP having intrinsic E3 ligase activity, in addition to its major chaperone function, and Figure 1C demonstration that whole-cell APP is associated with or directly modified by UBQ in the presence of CHIP. In Figure 2B, top panel, APP is pulled down with UBQ in the presence of CHIP (lane 3) or MG132 (lane 2), consistent with Figure 1C, panel 6 results. However, as shown in Figure 2B, third panel down (IP: CHIP, WB: UBQ), directly bound APP (panel 4) is not seemingly ubiquitinated (panel 3, lane 3) in the absence of MG132. There is an unexpected heavy pull-down of ubiquitinated proteins by the myc antibody in non-myc-transfected cells when MG132 is present (lane 2). Lane 4 results indicate that non-specific, and possibly APP bound to CHIP, ubiquitinations can be driven by general proteasome inhibition. Nevertheless, lane 3 result suggests, but does not prove, that CHIP is only an intermediate indirectly promoting APP ubiquitination. Finally, from experiments that show overexpression of CHIP stabilizes APP levels and accelerates complex formation, we reasoned that knock-downs of CHIP or chaperone Hsp70 should eliminate them. Indeed in Figure 2C and D IP experiments, drastic declines in CHIP or Hsp70 are shown to greatly diminish CHIP–APP and APP–Hsp70 as well as Hsp70–APP and APP–CHIP interactions, respectively.

Subcellular colocalization of βAPP_{751} and CHIP

Previous studies have shown that CHIP interacts with other proteins in the region of the ER (25,26,28) and that while found in the cytosol, it can localize to the nucleus during stressful stimuli (34). We utilized laser confocal microscopy to examine the distribution of both βAPP and CHIP in APP751-HEK cells. Cells were co-transfected with myc-tagged CHIP and expression plasmids for fluorescent protein constructs specifically targeting subcellular domains including the ER (pECFP-ER), Golgi complex (pECFP-golgi) and mitochondria (pEYFP-mito) (See Materials and Methods). Initial experiments aimed at localizing APP and CHIP produced a largely vesicular pattern of fluorescence with some perinuclear architecture (Fig. 3A). Using the specifically targeted compartment markers, we were able to co-localize the signals for CHIP and βAPP in the region of the ER and Golgi, but not in the mitochondria (Fig. 3B, C and D).

Proteasome inhibition enhances steady-state levels of APP and Hsp70

Environmental and misfolded protein stress in the cytosol triggers expression of the heat shock response, involving the induction of HSPs. HSPs are molecular chaperones that together with co-chaperones such as CHIP can stabilize or triage proteins for proteasomal degradation. Thus, degradation of fatally damaged proteins can be blocked by proteasome inhibition (39). By western blot analysis, we examined the impact of proteasomal inhibition and CHIP overexpression on HSP levels in APP751-HEK cells. MG132-treated cells showed a 2–3-fold increase in steady-state APP and Hsp70, as well as Hsp60 (Fig. 4A, lane 2 versus 1 or 3). In the presence of additional (exogenous) CHIP, compared with non-CHIP-transfected cells, this increase was further magnified (lane 4 versus 2). Interestingly, CHIP expression itself modestly stabilized steady-state APP levels (lane 3, top panel; see also Fig. 1C). Expression levels of Hsc70 and Hsp90 did not show significant changes. However, consistent with published results (34), CHIP is shown to upregulate levels of Hsp70 (and Hsp60 here). These findings suggest that in the presence of proteasome inhibition, APP

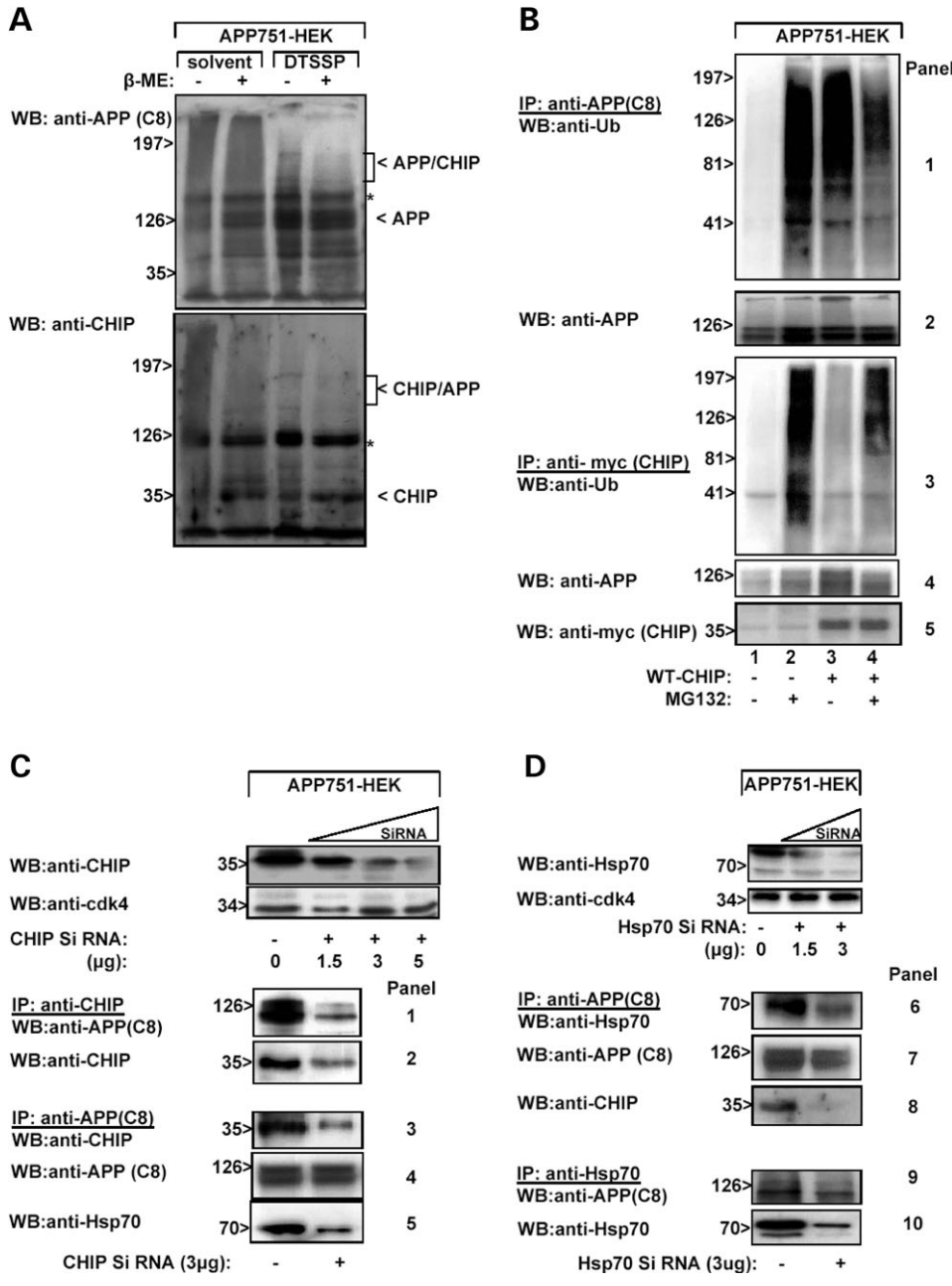

Figure 2. Functional characterization of CHIP–APP complex: (**A**) Cell lysates from APP751-HEK cells were subjected to protein crosslinking using DTSSP. Samples were mixed with the 2× SDS sample buffer with or without reducing agent (β-ME) and run on 6% SDS–PAGE. Western blots were probed with either rabbit polyclonal antibody for APP (C8, top) or CHIP (bottom). High molecular weight APP/CHIP complexes (bracketed) are suggested in lane 3, which are absent in presence of β-mercaptoethanol (lane 4). Asterisk denotes non-specific signals. (**B**) APP751-HEK cells were transiently transfected with myc-epitope-tagged CHIP plasmid and/or exposed to MG132 to determine the ubiquitination status of APP bound to CHIP. IP with anti-APP (C8) (top) or anti-myc antibodies (bottom) indicates that although UBQ associated with total APP is greatly increased by WT CHIP (top panel, lane 3), the pool of APP specifically bound to CHIP is not itself ubiquitinated (middle blot, lane 3). (**C** and **D**) CHIP Hsp70/APP interactions are sensitive to specific knock-down of endogenous components. APP751-HEK cells were transiently transfected with either CHIP siRNA (C) or Hsp70 siRNA (D). The upper panel of (C) shows the knock-down of expression by increasing dose of siRNA. Cdk-4 was probed as loading control. Same cell lysates were used for CHIP IP, and the reverse APP IP in the lower panels of (C) using anti-CHIP (panels 1 and 2) and anti-APP (C8) (panels 3–5) antibodies, respectively. Both reactions confirm the weakened interaction of CHIP with APP (panels 1 and 3) and APP with Hsp70 (panel 5) in the absence of CHIP (CHIP siRNA+). (D) Similar to CHIP experiment in (C), Hsp70 siRNA interferes with APP/Hsp70 (panels 6 and 9) and CHIP/APP (panel 8) complex formation.

accumulation is accompanied by an HSP response. Since βAPP and CHIP interaction is also upregulated by proteasome inhibition, HSPs, especially Hsp70, are predicted to partner in the complex. An examination of changes in transcript level of the various HSPs in response to proteasome inhibition in several cell types by semi-quantitative RT–PCR identified increases that largely correspond to the changes in protein noted by western blot (Fig. 4B).

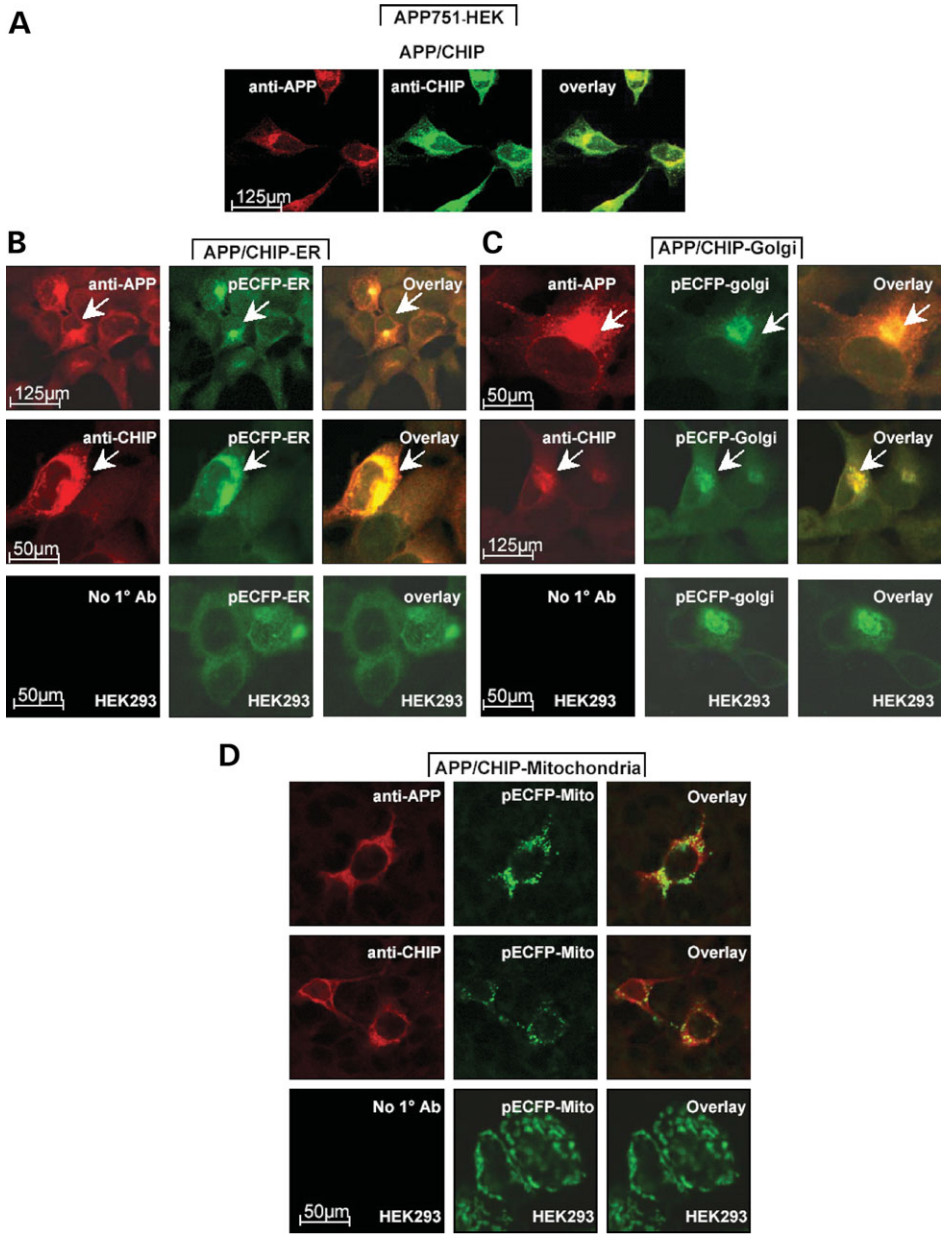

Figure 3. Subcellular co-localization of holo-βAPP$_{751}$ and CHIP. Confocal microscopy of APP-HEK cells expressing CHIP and other subcellular compartment-specific fluorescent proteins: pECFP-ER, pECFP-Golgi or pECFP-mito. (**A**) APP$_{751}$ and CHIP co-localize in vesicular compartments and in the perinuclear region. APP751-HEK stable cells co-transfected with CHIP were stained for APP 751 (anti-22C11; Cy2) and CHIP (anti-CHIP; Cy3). Single-optical sections were collected by confocal microscopy. In the absence of primary antibody, no signal was observed (not shown). Identification of specific compartments for APP and CHIP interaction using co-transfection with **(B)** pECFP-ER, **(C)** pECFP-Golgi and **(D)** pECFP-mito. APP and CHIP co-localize in the ER (B) and Golgi (C), with no evidence for their interaction in the mitochondrial compartment (D). All Figures represent a single-optical section collected in multi-tracking mode by laser confocal microscopy.

Interactions between holo-βAPP, CHIP and selected molecular chaperones

Previous studies have shown that the ER-associated chaperone Bip/Grp78 (a member of the Hsp70 chaperone family) interacts with βAPP to facilitate its correct folding and metabolism (2). We next investigated whether the βAPP and CHIP interaction incorporated several HSPs and whether they were differentially sensitive to MG132 treatment. Using lysates prepared from the APP751-HEK cell line, we find that stress induced by proteasomal inhibition leads to an increased association not only between CHIP and βAPP (as noted earlier), but also between CHIP and Hsp70 (Fig. 5A). A lesser change, but in the same direction, is noted in the interaction of CHIP/APP and Hsp60, following proteasome inhibition. These interactions are also identified when each

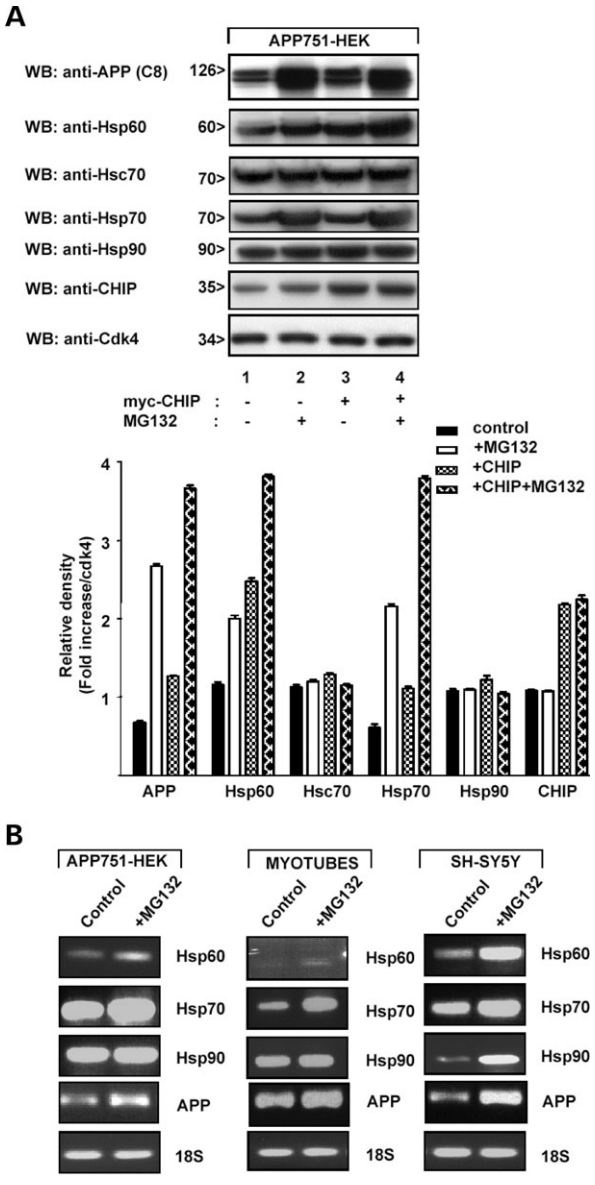

Figure 4. Effect of CHIP and proteasome inhibition on the expression of several molecular chaperones. (**A**) Western blots of whole-cell lysates from APP751-HEK cells with or without exogenous CHIP transfection in the presence or absence of proteasome inhibition. Equal amounts of each extract were fractionated on 10% polyacrylamide gels and blotted with the indicated antibody. Proteasome inhibition with MG132 increases steady-state levels of βAPP as well as Hsp70 and Hsp60 but not Hsc70 and Hsp90. Densitometric analysis corresponds to the western blot, and relative densities were obtained by normalizing cdk-4 ($n = 5, P < 0.05$). (**B**) Semi-quantitative PCR analysis of mRNA expression for βAPP and HSPs in the presence of proteasome inhibition. The ethidium bromide stained gel shows that MG132 treatment consistently increases Hsp70 levels. Lesser and much more mild increases are shown for APP, Hsp60 and Hsp90. Amplification of 18S RNA was used as a control.

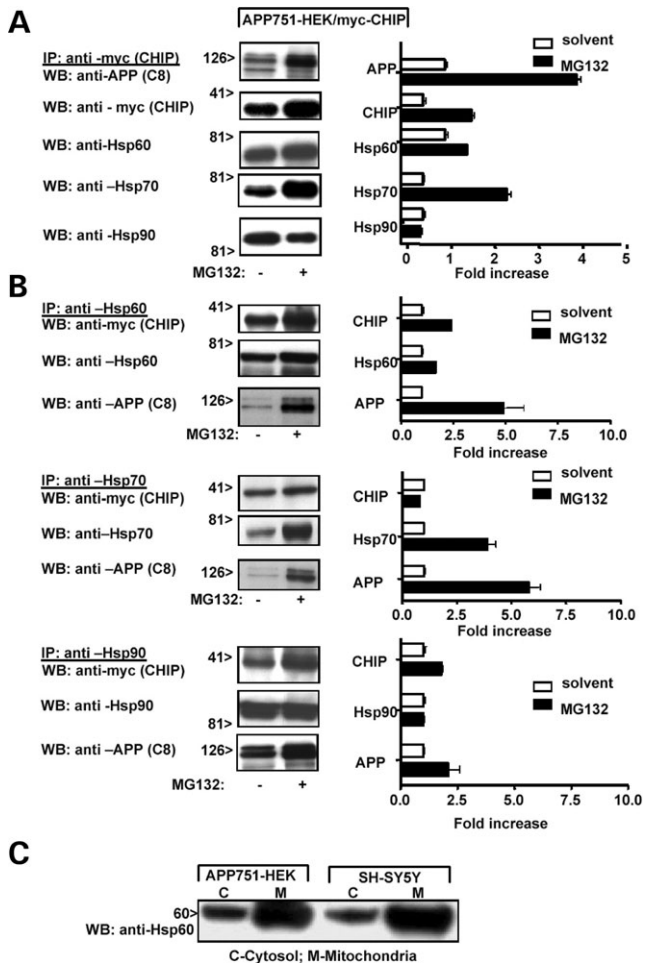

Figure 5. Interactions between APP, CHIP and selected molecular chaperones. IP experiments were used to identify associations between APP, CHIP and members of the heat shock family of proteins. (**A**) IP from APP751-HEK cells with anti-CHIP identifies associations with APP, Hsp 60, Hsp70 and Hsp90. All interactions increase in the presence of proteasomal inhibition except for Hsp90. The bar graph to the right displays the results of densitometric quantification (arbitrary units) for three independent experiments. (**B**) The same cell extracts were used for inverse IPs with antibodies against Hsp60, Hsp70 and Hsp90. The immunoblots identify the presence of the same interactions as seen in (A) and their enhancement following proteasomal inhibition. Results are expressed in fold increase with respect to MG132 untreated cells. (**C**) The level of mitochondrial Hsp60 expression in the cytosol versus mitochondria. Mitochondria and cytosolic fractions were isolated from APP751-HEK and SHSY5Y cells and resolved on 8% SDS–PAGE. The cytosolic fraction is shown to retain significant levels of Hsp60 ∼25% of mitochondrial levels.

of the inverse IP are performed (Fig. 5B). Hsp90 levels and associations did not appear to change much in this experimental paradigm. The association with Hsp60, considered a mitochondrial chaperone, is somewhat surprising. However, when checked (Figure 5C), significant levels of this protein were found present in the cytosol.

CHIP affects βAPP metabolism and associates with secretase products of its proteolysis

In order to understand what effect CHIP–APP interactions may have on holo-βAPP metabolism, we used a pulse-chase labeling paradigm. APP751-HEK cells were transfected with either a WT CHIP or a control GFP construct. After pulse labeling with a mixture of ^{35}S-methionine and cysteine, cells were chased for times up to 120 min. Extracts from each time point were immunoprecipitated with a rabbit polyclonal antibody directed against the extreme C-terminus of APP. The presence of transfected CHIP appears to stabilize

mature holo-βAPP (Fig. 6A graph and chart). This is consistent with the results of Figures 1C, 2B and 4A showing the modest inductive effect of CHIP on steady-state holo-βAPP levels. Transfection with CHIP did not have an impact on the appearance of C-terminus APP fragments (CTFs) of Figure 6B. CTFs in this molecular range are produced by the action of β- and α-secretases on APP to yield C99 and C83 amino acid species (12–10 kDa), respectively. As expected, in the presence of MG132, there is accumulation of both CTFs, which shows further stabilization in cells that co-express CHIP (Fig. 6B). In order to determine whether these proteolytic products of APP also associate with CHIP and/or HSPs, we utilized IP assays (Fig. 6C). Extracts were prepared from APP751-HEK cells transfected with CHIP, treated with MG132, or both. First, IP with anti-CHIP, -Hsp60, -Hsp70 or -Hsp90, followed by western development with an antibody directed against APP, confirms an association between all of these molecules. However, only CHIP–APP and Hsp70– or Hsp60–APP interactions are enhanced, following proteasomal inhibition (Fig. 6C, upper panel). In Figure 6C, lower panel, it is shown that an interaction between the CTF C99, the precursor to Aβ, and Hsp70 is slightly stronger than with the others. The specificity is determined by detection with both anti-C8 (recognizing all CTFs, upper panel) and antibody 6E10 (recognizing the Aβ1–17 epitope within C99, lower panel). This association is brought out only in the presence of CHIP with MG132. Interestingly, although Hsp90 is also pulled down with βAPP (Figs 5B, bottom, and 6C, far right), it is not involved with CTFs. These results identify differential associations between CHIP, certain HSPs and βAPP, and that proteolytic products of βAPP are also detected in the complex but only if stabilized by proteasome inhibitors.

In its role of co-chaperone, CHIP is expected to stabilize proteins when faced with oxidative stress and potential irreversible damage. We tested this in cell culture exposed to hydrogen peroxide (H_2O_2). In Figure 6D, increasing doses of H_2O_2 resulted in declining levels of βAPP. The overexpression of CHIP (+) significantly interrupted degradation of βAPP, as predicted.

CHIP and HSP interactions with $A\beta_{1-42}$

The results so far show involvement of CHIP in the stabilization of holo-βAPP and implicate CHIP in the proteasome-sensitive disposition of secretase products of βAPP proteolysis. Hsp70 features prominently in both the processes. We next tested the hypothesis that CHIP and HSPs might also influence the levels and stability of the β-amyloid peptide. For these experiments, we utilized the human neuroblastoma cell line SH-SY5Y and a doxycycline-inducible adenoviral construct encoding $A\beta_{1-42}$. The latter is targeted for processing through the ER-Golgi system (14). Cultures were individually infected with adenoviral (Ad) constructs encoding CHIP, Hsp60, Hsp70 or Hsp90 and 24 h post-infection were co-infected with AdTREAβ_{1-42}; 24 h after this second infection, Aβ expression was induced by the addition of 1 μg/ml of doxycycline for 24 h. In the presence of Ad-CHIP expression, the accumulation of intracellular Aβ is substantially reduced compared with control (Fig. 7A, lane 4 versus 6). Extending this analysis to the HSPs, we found that there was a differential impact of HSP overexpression on the accumulation of $A\beta_{42}$. In Figure 7B, Hsp70 expression is shown to reduce accumulation of $A\beta_{42}$ (lane 4 versus 2), whereas Hsp60 had no effect (lane 6) (40). Interestingly, Hsp90 showed the greatest impact on $A\beta_{42}$ reduction (lane 8). The latter is an unexpected finding since Hsp90 is neither sensitive to proteasome inhibition nor associated with APP CTFs. The data from three additional independent experiments confirm these effects on Aβ-levels (Fig. 7B, chart).

These data raise the question of whether or not changes to Aβ levels are reflected in any way by the association of the same chaperones with the Aβ molecule. To address this, we immunoprecipitated each chaperone before probing western blots with anti-Aβ 6E10. Indeed, as shown in Figure 7C, Aβ is pulled down with endogenous Hsp70 (lane 2). Moreover, overexpression of Hsp70, by driving down total Aβ-levels (Fig. 7B), is correspondingly associated with lesser amounts (lane 4). Similarly, IP of endogenous CHIP yielded Aβ, and CHIP overexpression in turn was associated with a further reduction in attached Aβ (Fig. 7D). Endogenous Hsp90 is also avidly associated with Aβ. When overexpressed, Hsp90 similarly pulled down less Aβ (Fig. 7E), explained by its superior ability to lessen the total cellular load of Aβ (Fig. 7B). The importance of CHIP and HSP chaperone interactions with Aβ in a cellular context is emphasized in Figure 7F. Quantitative IP of Aβ from media and whole-cell lysates clearly demonstrates preponderance of intracellular over extracellular Aβ species in all the cell lines (see legend). Therefore, these chaperones display a variable capacity for interaction with and reduction of $A\beta_{42}$ load, which is only partially reflected in their interactions with APP CTFs and, in the case of CHIP, in their effects on APP metabolism.

CHIP accelerates $A\beta_{1-42}$ removal and protects against toxicity

The interaction of CHIP with APP and between CHIP and Aβ, taken with the CHIP-regulated reduction in steady-state Aβ levels, suggest that CHIP may (i) promote secretory processing and protease degradation or affect transcription control of βAPP, (ii) impose a block on β- and γ-secretase actions or (iii) hasten Aβ clearance. The first two possibilities are unlikely given the results presented thus far. Using a pulse-chase labeling paradigm, we then examined the degradation of Aβ in the stable APP751-HEK cell line in the presence and absence of added WT CHIP. Extracts were immunoprecipitated using antibody R1282 against $A\beta_{1-42}$ at varying times of chase (Fig. 8A). In the presence of exogenous CHIP, we have found that the rate of intracellular Aβ degradation is enhanced (Fig. 8A, graph). We next examined the functional effects of CHIP and HSPs on cell viability under stress from Aβ accumulation. SH-SY5Y cells were infected with various adenoviral constructs, as described previously. For all of the chaperones tested, there was a protective effect (60–80% increase) on cell viability as measured by 3-(4,5-dimethylthiazol-2-yl)-2,5-diphenyl-tetrazolium bromide (MTT) reduction levels (Fig. 8B). The combination of Hsp70 and CHIP was noticeably cooperative in this respect. We extended these findings to cultures of mouse primary cortical neurons, where CHIP (or Hsp70, not shown) increased the survival of cells challenged by Aβ accumulation. A corresponding decrease in the

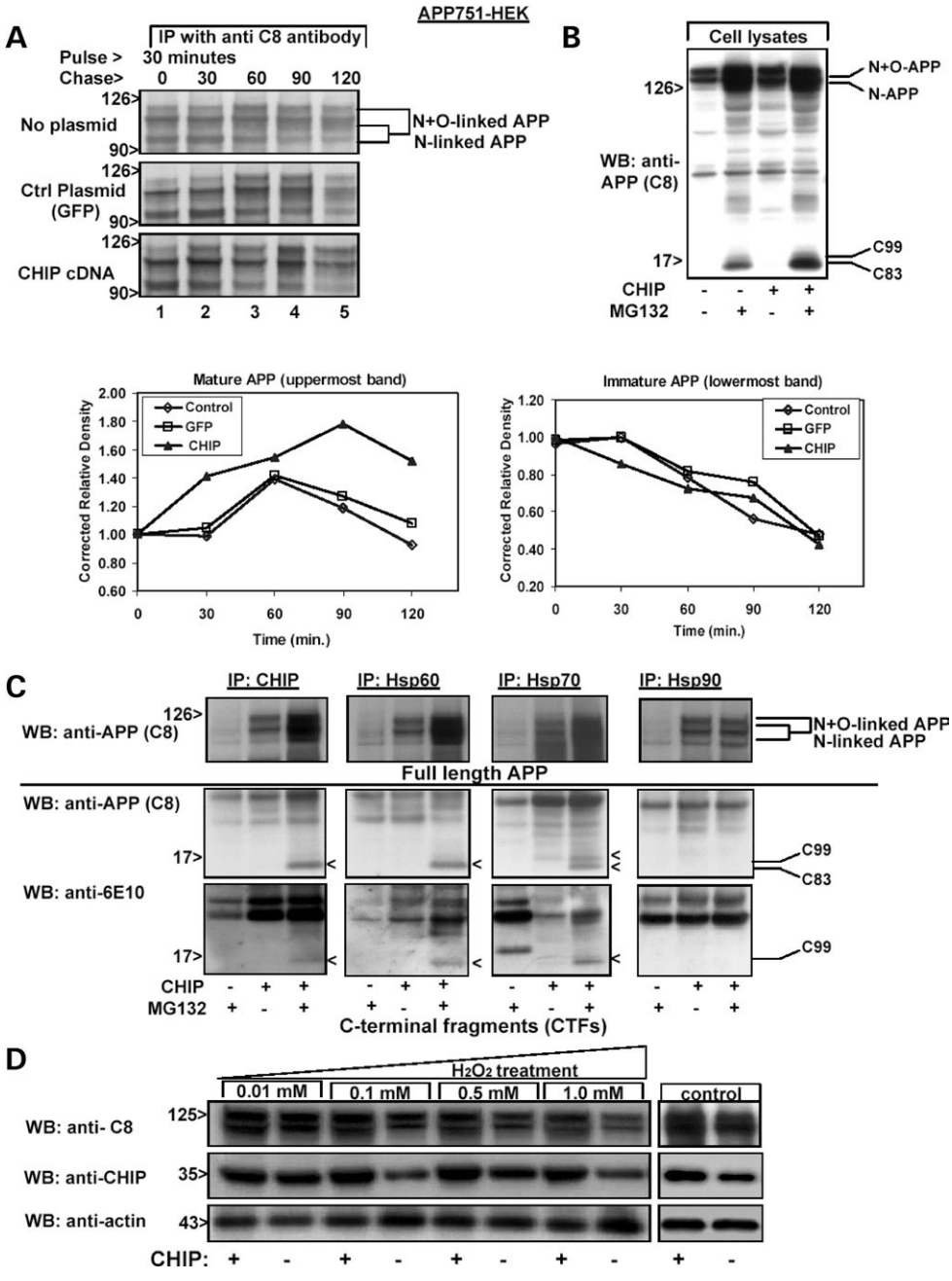

Figure 6. Functional effects of WT CHIP on β-amyloid precursor protein (βAPP) metabolism under normal and oxidative stress condition. (**A**) Pulse-chase analysis of APP maturation and degradation. APP751-HEK cells were transfected with WT CHIP or pEGFP or mode transferred with no added DNA. Cells received a 30 min pulse labeling with ^{35}S-met/cys and then were chased for the indicated time periods. Cell extracts were immunoprecipitated with polyclonal anti-APP antibody C8. The 2positions of differentially glycosylated forms of APP are indicated. Samples were electrophoresed on a 4–12% Bis–Tris gel (Invitrogen) and then treated for autoradiography. The plot below gives the densitometric analysis of control (open diamond and square) versus CHIP-expressed (open circle) samples. The relative values for mature APP (left graph) within each of the three conditions were first normalized to their respective immature APP signal at time 0 and then with respect to each other. Immature APP signals (right graph) for each of the conditions were normalized to their respective time 0 value (set at 1.0). (**B**) Cooperative CHIP expression and proteasomal inhibition enhance APP-CTF accumulation. Western blot analysis of Triton-X100 soluble fraction from APP751-HEK cells transiently transfected with WT CHIP. In the presence of MG132 treatment, levels of CTFs are increased, an effect that is further enhanced by CHIP overexpression. (**C**) IPs above and immunoblots to the left as indicated were used to explore APP and CTF's interactions using proteasome inhibition, or both are shown to enable detection of APP CTF interactions using antibodies C8 and 6E10. CHIP, Hsp60 and Hsp70, but not Hsp90, associate with both the C99 and C83 APP-CTFs as detected by antibody C8. The identity of C99 is verified by stripping and re-probing with antibody 6E10. (**D**) APP751-HEK cells were transfected with WT CHIP or empty vector and subjected to oxidative stress using increasing doses of hydrogen peroxide for 1.5 h. Whole-cell lysates were probed by western blot for anti-APP, anti-CHIP and anti-actin. CHIP increases the reduction in steady state of APP levels, caused by increasing H_2O_2 concentration.

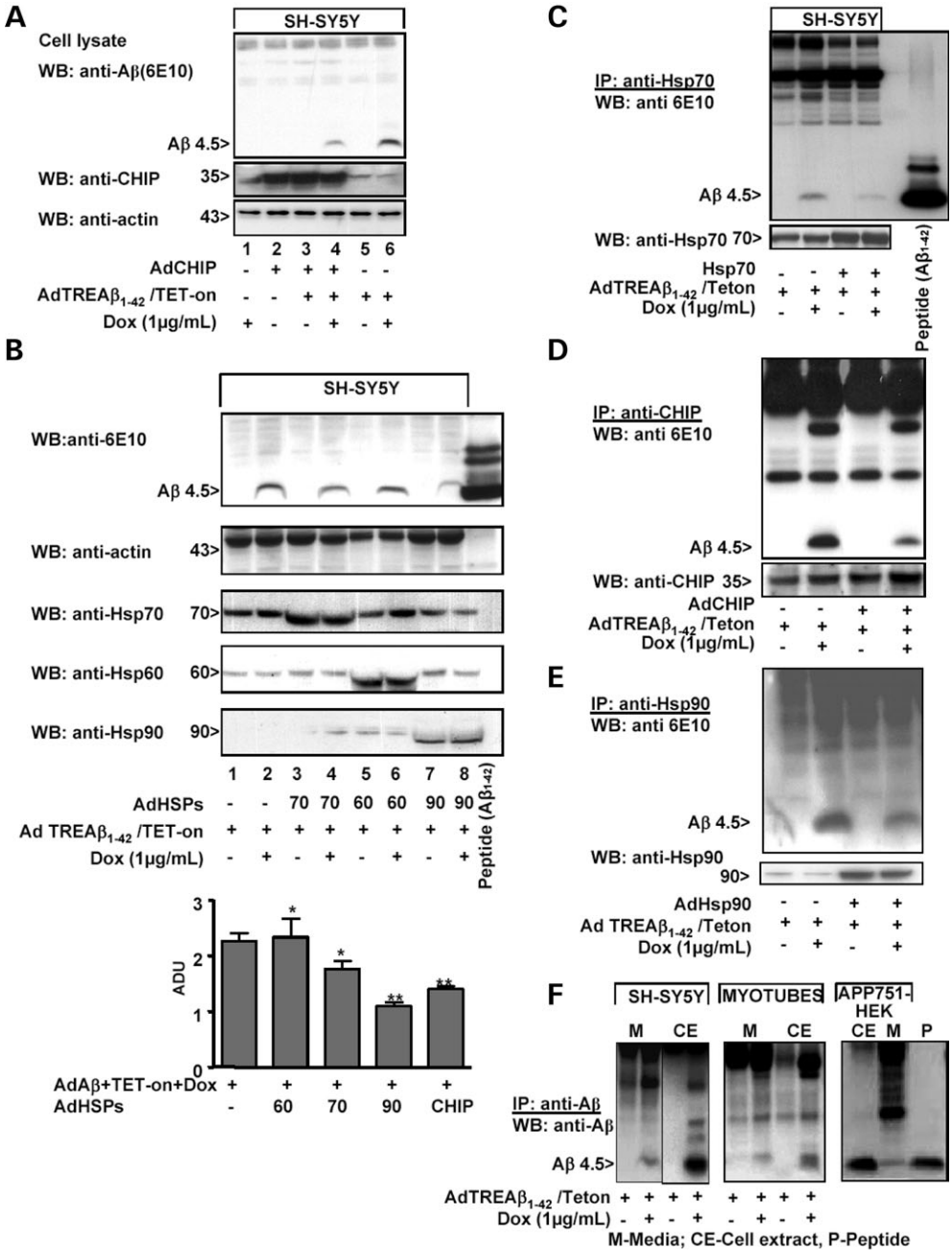

Figure 7. Interactions between CHIP, HSPs and β-amyloid and their effects on β-amyloid accumulation. SH-SY5Y neuroblastoma cells were infected with the doxycycline-inducible adenovirus encoding β-amyloid and induced in the presence or absence of exogenously expressed molecular chaperones. (**A**) Western blot analysis shows that overexpression of CHIP–adenovirus attenuates the accumulation of intracellular Aβ (lane 4 versus 6). (**B**) Overexpression of other molecular chaperones also reduce Aβ accumulation. Western analyses demonstrate that Hsp70 and Hsp90 reduce steady-state Aβ levels (lanes 4 and 8 versus 2). Densitometric analysis of several experiments is shown below. (**C**–**E**) ADU, arbitrary densitometric units. IP with anti-Hsp70 in (C) and with anti-CHIP in (D) or with anti-Hsp90 in (E) is followed by immunoblot using with antibody 6E10 (versus Aβ). An interaction between these molecular chaperones and Aβ is shown. Overexpression of Hsp70, CHIP and Hsp90 reduce the pull-down of Aβ. The results corrected with reductions in the steady-state accumulation of cellular Aβ shown in (A) and (B). (**F**) The results of adenovirus- mediated $Aβ_{42}$ expression show robust intracellular β-amyloid accumulation in all cell types. SH-SY5Y and myotubes were infected with the adenovirus-encoding β-amyloid and induced in the presence of doxycycline. Equivalent amounts of whole-cell extract (100 μg) and the total media (35 mm dish, 1 ml) of the infected and uninfected APP751-HEK cells were used for IP by R1282 (for Aβ), followed by immunoblot using antibody 6E10 as probe. The very last lane corresponds to a synthetic peptide control added to sample buffer.

detectable levels of Aβ peptide is shown beneath Figure 8C. Hsp90 resulted in a similar reduction in levels of endogenous Aβ in primary cortical neurons, whereas Hsp60 did not (not shown), consistent with the SH-SY5Y cell results presented in Figure 7B. These data demonstrate that manipulation of UBQ ligases and/or the expressions of their molecular chaperones may provide cells with a strategy to combat cellular stress associated with β-amyloid accumulation.

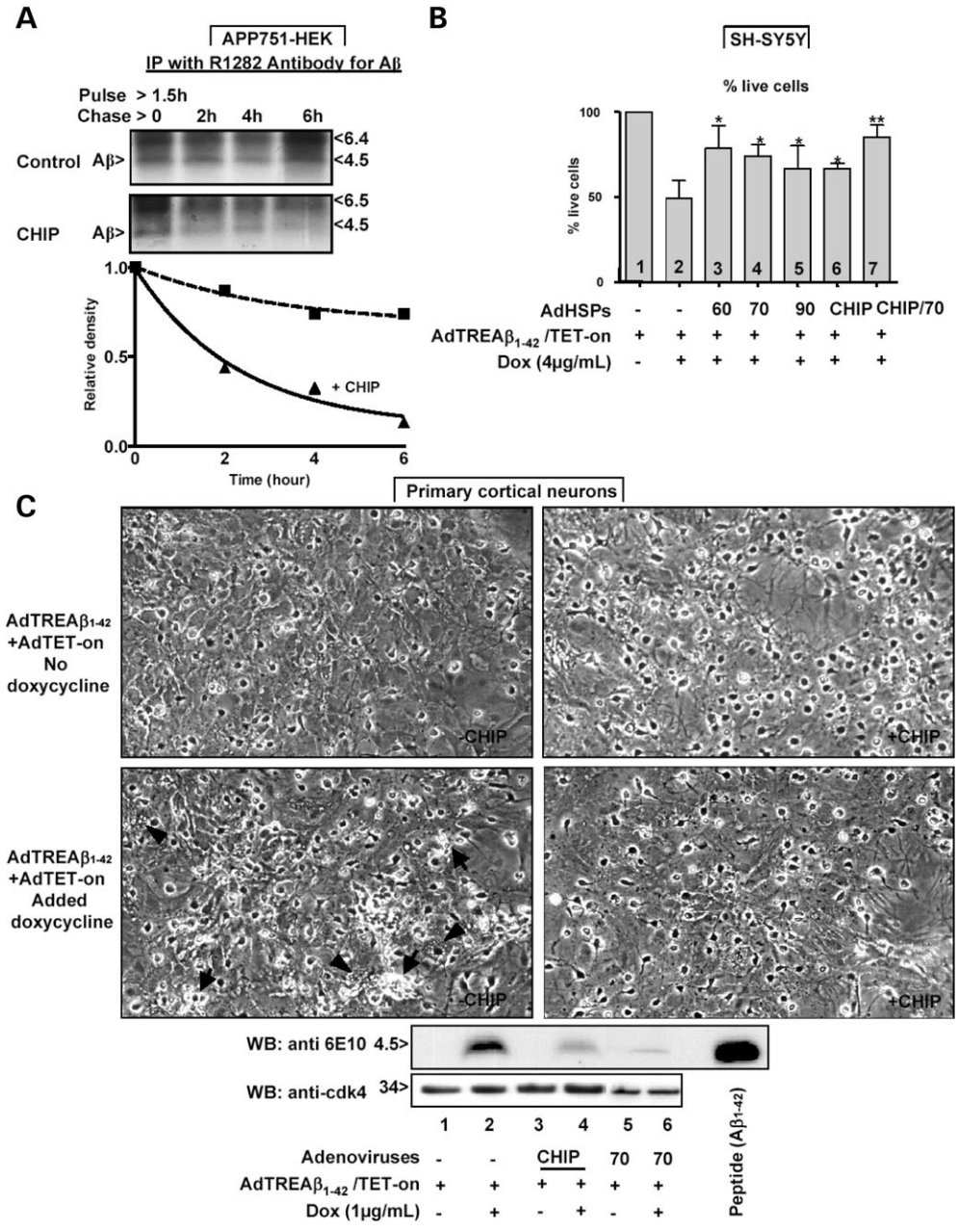

Figure 8. Effects of CHIP on Aβ metabolism and toxicity. (**A**) APP751-HEK cells were transiently transfected with WT CHIP. Cells were pulse-labeled for 90 min with ^{35}S-met/cys and then chased for the times indicated. Cell extracts were immunoprecipitated using polyclonal antibody R1282 against $A\beta_{42}$. Migration of cellular Aβ is indicated. Densitometric analysis of Aβ is plotted for control (rectangle) and CHIP-expressing samples (triangle) showing enhanced rate of Aβ degradation. All values were normalized to the 0 time points. (**B**) Summary of MTT assay results shows that adenoviral-transduced chaperone expression protects SH-SY5Y neuroblastoma cells against Aβ-induced cell toxicity. All bar samples represent the mean ± SEM for $n = 3$ experiments, each performed in triplicate. Values normalized to non-Aβ-expressing cultures in bar 1. (**C**) Protection of primary cortical neuron cultures from Aβ-induced cell death by overexpression of CHIP and Hsp70. Cultures were infected with/without Ad-CHIP viruses 24 h prior to infection with $AdTREA\beta_{42}$. All fields were photographed through a 40× phase-contrast objective, 24 h after doxycycline induction of amyloid expression (arrowhead: vacuolar degeneration; arrow: cell rounding). Western blot analysis of the same cultures as in (C) showing a marked decrease in levels of intracellular $A\beta_{42}$ in the presence of CHIP and Hsp70 overexpression.

DISCUSSION

Several studies have highlighted the close association between molecular chaperones, co-chaperones and the UBQ-proteasomal degradation pathway to influence the handling of misfolded, unfolded or aggregated proteins (41–43). CHIP is one such co-chaperone, which is endowed with dual properties and sensor function to switch between protein stabilization and degradation pathways. Thus, CHIP acts as a co-chaperone regulating correct folding (16) and as an E3

UBQ ligase (21,44). Owing to this contrasting bifunctionality, CHIP appears to triage protein fate between the chaperone and proteasome systems (22–24). Although CHIP has been suggested to play a widespread role in protein handling among polyglutamine disorders, Parkinson's disease and tauopathies (13,25,30–32), there is no previous description of any contribution to APP biology. In the present study, we have presented data that support a direct interaction between WT holo-βAPP and CHIP. IP and western blot interaction studies were performed in several endogenous expression systems. In C2C12 myotubes, for example, using a native CHIP antibody, it is shown that SDS-stable CHIP–APP complexes are readily pulled down. Although CHIP levels themselves do not greatly change, levels of normal APP, a potential client protein, are greatly stabilized in the presence of proteasomal inhibition and the amount of precipitable complex increases proportionately (Fig. 1A). In the overexpression system (stable APP751-HEK), IP/WB experiments also reveal that CHIP is interacting with both N- and N + -O-linked glycosylated APP isoforms. Moreover, APP/endogenous CHIP complexes are captured in the absence of MG132 using a protein crosslinker.

The expected engagement of UBQ in the APP–CHIP complexes is shown in several ways. First, APP–UBQ interactions are stabilized under proteasome blockade. Secondly, APP–UBQ associations are also increased when WT CHIP is overexpressed. Thirdly, a mutant CHIP lacking the RING-finger containing UBQ ligase domain (ΔUBL) does not result in the ubiquitination of APP. Next, we show that the APP directly attached to CHIP is not itself ubiquitinated, suggesting another E3 ligase is subsequently involved in APP ubiquitination. Finally, APP/CHIP complex formation is reduced when CHIP or Hsp70 are knocked down. Importantly, these interactions are not limited to cell culture systems, as we have found evidence for molecular association between CHIP and βAPP in samples prepared from post-mortem human brain. Our model of CHIP's bifunctional triage action is illustrated in Figure 9. In summary, CHIP may switch roles to (i) stabilize normal APP levels or (ii) act as an intermediate in the ubiquitination of an unwanted, smaller pool of APP (probably targeted to the proteasome) and additionally to (iii) reduce levels of cytotoxic β-amyloid. The functional significance of CHIP as chaperone to stabilize APP during oxidative stress is demonstrated in Figure 6D.

Previous studies by Nunan *et al*. (36,37) found that C-terminal fragments of APP generated by β-secretase action (e.g. APP–CTFβ or C99) are ubiquitinated and subjected to cleavage in a proteasome dependent manner. Little else is known of holo-βAPP metabolism by the proteasome, whereas Aβ peptides are stabilized by proteasome inhibition (45,46). On the contrary, more is known about βAPP movement through the secretory pathway, endosomal recycling, secretase processing and lysosomal degradation (47–54). In support of chaperone-mediated APP processing, Yang *et al*. (2) found that APP and the ER stress response chaperone Bip/Grp78 interact to facilitate the correct folding of nascent APP. They also demonstrated that APP underwent β/γ secretase processing in the ER/Golgi complex and that Bip/Grp78 overexpression resulted in reductions of soluble APP, CTFs and Aβ peptides. The combined published UBQ-proteasome and chaperone data suggested that βAPP biology, folding and degradation might also be subject to the regulation by a bifunctional co-chaperone/UBQ ligase such as CHIP. Here, we have shown that CHIP, along with the chaperones Hsp60, 70 and 90 not only interact with but also influence the metabolism of holo-βAPP.

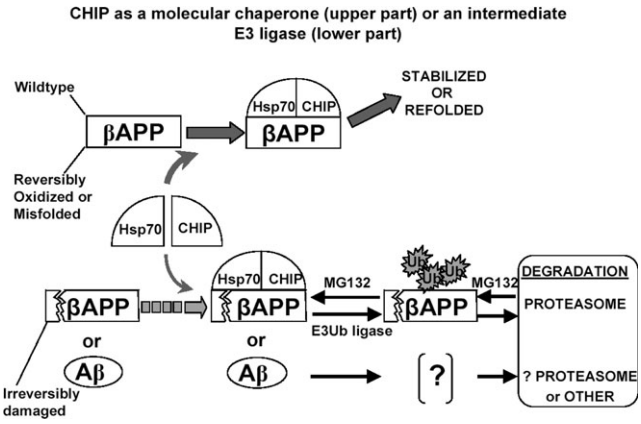

Figure 9. A model of CHIP in the biology of β-APP homeostasis. CHIP is endowed with bifunctional properties as a molecular chaperone (top) and as an intermediate to another UBQ E3 ligase (bottom). CHIP may stabilize, protect or re-fold either normal or salvageable holo-APP in most circumstances (strong arrow). However, where some APP is destined for destruction or in case of β-amyloid accumulation (light and broken arrow), CHIP will assist in APP ubiquitination or other pre-degradation reactions. Another E3 ligase is presumed to take over the direct ubiquitination reaction after CHIP.

The results from pulse-chase experiments suggest that although CHIP may stabilize APP for up to 90 min into the chase, it is thereafter processed at a rate comparable with that observed under control conditions. We note that degradation rates of α-synuclein in the presence and absence of CHIP also become similar (27). This is consistent with the stabilization or maintenance of steady-state levels of WT APP in the presence of CHIP (Figs 1C, 4A and 6B). Further evidence for involvement of CHIP and the proteasome system in APP handling comes from our finding that in addition to CHIP–APP complex formation, Hsp70–APP and CHIP–Hsp70 interactions are specifically stabilized in the absence of proteasome function (Fig. 5A and B). Interestingly, CHIP also influences APP C-terminus fragment levels and is itself bound to them, an effect made detectible when the proteasome is blocked. As these fragments include the β-secretase-generated C99 fragment (the immediate precursor to Aβ), especially as shown in Hsp70 pull-downs in Figure 6C, it suggested that molecular co-chaperones, such as CHIP, might also influence the accumulation of the β-amyloid peptide product of subsequent γ-secretase action on C99.

Although the pull-down data show CHIP, APP and the HSPs co-exist in a soluble complex (Fig. 5A), their relative stoichiometry and strength of binding remain to be determined. The 150 and 190 kDa crosslinked complexes of Figure 2A could indicate that CHIP–APP may either interact directly and independent of HSP or be tethered by a bridging chaperone, i.e. Hsp70 in 1:1:1 molar ratio. We favor an interdependent trimolecular arrangement because the siRNA data show that the

APP–Hsp70 partnership depends on CHIP as much as APP–CHIP depends on Hsp70 (Fig. 2C and D). Owing to the fact that HSP/CHIP interacts with APP–C99 CTF (Fig. 6C) and the Aβ peptide (Fig. 7C and D), it is tempting to speculate that binding to holo-APP involves the intact Aβ domain. Future interaction experiments with various deletion constructs will address this question.

The selective complex formation between CHIP and APP, which exhibits protesome dependence and involves Hsp70 over the other HSPs, is additional evidence in favor of a specific role of CHIP in APP processing. We previously have shown that Hsp70 is upregulated as part of the stress response to intracellular Aβ accumulation in cultured neurons (14,15). In this context, it is important to note that yet another role of CHIP is to activate HSF-1, which positively controls the expression of Hsp70 (34,35). In our study, Hsp70 (and Hsp60) levels are also induced, although modestly in the presence of exogenous CHIP (Fig. 4A). Conversely, CHIP controls Hsp70 levels by orchestrating its proteolytic destruction once the misfolded or unfolded protein substrate is disposed of or refolded ('stress recovery' or 'sensor switch function') (35). Indeed, Hsp70 protein levels were the most responsive to MG132-mediated proteasome inhibition and more so with added CHIP (Figs 4 and 5). Levels of Hsp70 transcripts also become elevated after proteasome blockade (Fig. 4B). The proteasome inhibitor MG132 is a peptide aldehyde that accelerates the transcription of HSPs and other ER chaperones. Thus, under proteasome blockade, intracellular protein breakdown is inhibited by ~70%, triggering the expression of heat shock genes, or components of the proteolytic pathway such as polyubiquitin (39). Our data in Figures 1C and 4 are consistent with this. The precise steps in the degradation of the proteasome-sensitive pool of βAPP and in the subsequent termination of Hsp70 levels that are orchestrated by CHIP, if resembling the model of protein stress (35), remain to be investigated. Whether APP and Hsp70 compete in anyway for CHIP function and confirmation that CHIP does not itself directly ubiquitinate APP are also questions for future study.

We report for the first time that there additionally exists an interaction between CHIP and other HSPs, with the more toxic APP byproduct, the $A\beta_{1-42}$ peptide. We also show here that CHIP, Hsp70 and Hsp90 attenuate the accumulation of $A\beta_{1-42}$. The relationship between the interaction of CHIP with β-APP and additional capacity to depress steady-state Aβ levels (Fig. 7A) is not explained by an inhibition of or sequestration of APP from secretase processing. First, CHIP expression increases rather than decreases the appearance of the MG132-stabilized C-terminal fragments (Fig. 6B and C). Secondly, pulse-chase results suggest that CHIP promotes Aβ degradation (Fig. 8A). We found that Hsp70 expression equally degrades steady-state Aβ levels (Fig. 7B), an effect probably related to its strong interaction with CHIP and APP, as shown in Figure 5A and B, respectively, under proteasome blockade.

Not all the HSPs act similarly in our CHIP/APP/Aβ paradigm. Although, Hsp90 is also a CHIP client chaperone (Fig. 5), it appears not subject to the same proteasome regulation and APP binding, as are Hsp70 and, to a lesser extent, Hsp60, in various cell types (Figs 4 and 5A and B). We speculate this might be related to its association with an even greater reduction in Aβ levels and decreased affinity for the APP-CTFs. CHIP as mentioned, hastens the proteasome-dependent degradation of Hsp70 when stress protein levels fall below a threshold (35). Whether Hsp90 escapes such controls remains to be found. As shown in Figure 7, all the HSPs tested interact with Aβ. Moreover, the ratio of associated Aβ to HSPs decreases in most cases as the individual HSP levels are increased, as expected. The exception, Hsp60, does not affect Aβ levels to the degree the others do [Fig. 7B and (40)] but is nevertheless highly protective via an alternative mitochondrial mechanism [Fig. 8B and (40)]. Although Hsp70 is closely linked to CHIP and proteasome clearance, the Hsp90 and Hsp60 results highlight the probability that differential chaperone mechanisms exist for the regulation of Aβ.

The functional consequence of CHIP and HSP action to depress Aβ levels on cell viability was demonstrated in two neuronal culture systems and by two assays: either CHIP or Hsp70 alone and synergistically, protected SH-SY5Y cells from intracellular Aβ stress. In primary neurons, Hsp70 (and Hsp90) or CHIP expressions also rescued cells from Aβ toxicity in step with reductions in Aβ levels (Fig. 8). Increasing evidence supports the hypothesis that many neurodegenerative conditions have in common cellular stress associated with protein misfolding, differential partitioning and/or aggregation. Here we found that the bifunctional co-chaperone/E3 UBQ ligase CHIP, in association with molecular chaperones, especially Hsp70, affects the biology of a new client substrate, βAPP, and concurrently enhances the removal of its toxic proteolytic product. Another neurodegeneration-linked protein, phospho-tau, is a client substrate for CHIP. Similar to our data on APP, the protein tau, CHIP and HSPs are in complex together. The resulting direct ubiquitination of tau is also enhanced in the presence of MG132 (12,31,32,55). In the APP instance, the difference is that CHIP probably acts as the intermediate before the transfer to another ligase for direct ubiquitination.

It is curious that CHIP has not been reported in yeast two hybrid screening assays using βAPP as bait. Further studies will address whether this interaction preferentially takes place in insoluble or inaccessible compartments. Any role of Parkin in the βAPP–CHIP interaction also needs to be clarified in future research. In this light, CHIP may conceivably pass APP (or Aβ) onto Parkin, much like the PAEL-R substrate (26,56), or have no relation to Parkin as in the case with tau (12,32).

MATERIALS AND METHODS

Constructs and reagents

Plasmids encoding full-length, myc-epitope-tagged WT CHIP in pcDNA3.1 (GenBank™ accession CHIP IMAGE clone ID: 3847704 ATCC) and various deletion mutants in the U-box region were generated as described (57). HEK293 cells stably transfected with human APP751 (APP751-HEK) were cultured in the presence of G418, as described previously (58). Adenoviral constructs for Hsp60, Hsp70 and Hsp90 were as described previously (59). Adenoviral construct for

CHIP and affinity purified, rabbit anti-CHIP was as described in Dai *et al*. (34). The subcellular localization expression constructs pECFP-ER, pECFP-golgi and pEYFP-mito were from Clontech (Mountain View, CA, USA). Rabbit antibodies C-8 versus the C-terminus of human APP and R1282 versus Aβ42 were kindly provided by Dr D. Selkoe (Harvard Medical School, Boston, MA, USA). Antibodies against Hsp60, Hsp70 and Hsp90 were purchased from both StressGen (San Diego, CA, USA) and Santa Cruz Biotechnology (Santa Cruz, CA, USA). Anti-calnexin, anti-Grp94, anti-phospho PERK, anti-insulin receptor (alpha), anti-Grp94 and anti-UBQ (P4D1) were from Santa Cruz Biotechnology. Polyclonal anti-CHIP and monoclonal anti-myc tag (9E10) were purchased from Upstate Biotechnology (Lake Placid, NY, USA). Mouse anti-APP (22C11) was from Chemicon and monoclonal anti-β-amyloid (6E10) was purchased from Signet Pathology Systems (Dedham, MA, USA). Proteasome inhibitors MG132 and Lactacystin were purchased from Calbiochem (LaJolla, CA, USA). Human brain samples were kindly provided by the Harvard Brain Tissue Resource Center (McLean Hospital; Harvard Medical School; Belmont, MA, USA).

Transient and siRNA transfection All cell lines were transiently transfected using a calcium phosphate precipitation method (2M $CaCl_2$, DNA and water plus 2× HBS). Cells were treated 48 h after transfection with either 30 μM MG132 or Lactacystin for an additional 12 h. APP751-HEK stably cells were transfected with either CHIP SiRNA (Santa Cruz) or Hsp70 SiRNA, as described previously (15). Cell lysates were used for western blot analysis and for IP experiment.

Protein crosslinking experiment A crosslinker agent 3,3′-dithiobissulfosuccinimidyl propionate (DTSSP) was used as per the manufacturer's protocol (Pierce, Rockford, IL, USA). Cell lysates (100 μg) from APP751-HEK stable cells were exposed to a molar excess of DTSSP or solvent. The mixture was incubated on ice for 2 h after which the reaction was quenched with 50 mM Tris, pH7.5, for 15 min on ice. Samples were mixed with 2× SDS sample buffer with or without β-mercaptoethanol (β-ME) and resolved on 6% SDS–PAGE, transferred, incubated with appropriate antibodies and the signals visualized using enhanced chemiluminescence reagents and film from GE Healthcare (Piscataway, NJ, USA).

Mitochondrial and cytosolic fractionation We used a method to isolate the mitochondrial and cytosolic fraction from cell lines, as described previously (40). Cells were suspended in ice-cold sucrose–mannitol buffer, followed by homogenization in a Dounce homogenizer. Homogenates were centrifuged at 600*g* for 5 min at 4°C. The supernatant containing the mitochondria was saved, and the procedure repeated on the pellet. The pooled supernatant was centrifuged at 16 000×*g* for 10 min at 4°C. The new pellet containing the mitochondria was resuspended in 100 μl isolation buffer (Pierce Biotechnology). The supernatant is the cytosolic compartment.

Infection of primary cortical neurons and SH SY5Y cells with adenovirus Low passage SH-SY5Y cells were grown to 70–80% confluence in DMEM containing 10% FBS, penicillin–streptomycin, 1 mM pyruvate and 2 mM glutamine. Primary cortical neurons were isolated and cultured in Neurobasal medium plus B27 supplements (Invitrogen), as previously described (14). Unless otherwise indicated, cells were first infected for 24 h with Ad-CHIP, AdHsp60, AdHsp70 or AdHsp90 constructs (50–100 m.o.i.) and then subjected to a second infection for an additional 24 h with AdTet-On and AdTRE-Aβ42 (1:5 ratio). Aβ expression was induced by the addition of doxycycline at 1 μg/ml for a further 24 h.

Immunoprecipitations

Cells were lysed in Triton lysis buffer containing Tris–HCl (pH 7.4, 20 mM), NaCl (150 mM), $Na_4P_2O_7$ (10 mM), Na_3VO_4 (2 mM), protease inhibitor cocktail (Complete; Roche Biochemicals, Indianapolis, IN, USA), phenylmethylsulfonyl fluoride (44 μg/ml), and Triton X-100 (1% vol/vol), incubated on ice for 10 min, and then centrifuged at 10 000*g* for 10 min. The whole-cell extract supernatants were used directly for western blot analysis (20 μg of total protein) or for IP. IPs were performed using 100–300 μg of extract protein. Following a preclearing incubation with protein A/G-Sepharose (Sigma, St Louis, MO), extracts were incubated for 3–4 h at 4°C with 3 μg of primary antibody, followed by the addition of Protein A/G Sepharose and an additional incubation at 4°C for 1 h. Immunoprecipitates were harvested by centrifugation at 14 000*g* for 5 min at 4°C and washed several times in 4°C 1× phosphate buffered saline (PBS) buffer containing protease inhibitor cocktail (Roche Biochemical) and PMSF before elution and electrophoresis.

Western blot analysis

Protein (20 μg) from Triton-soluble cell extracts or immunoprecipitates were heated (95°C, 10 min) in Laemmli sample buffer, cleared by centrifugation, separated on SDS–PAGE and then blotted onto PVDF membrane (Immobilon-P; Millipore, Bedford, MA, USA). Membranes were blocked using TBS containing 5% (wt/vol) non-fat dry milk. After incubation with primary antibodies (1:500–1000 dilution) in the same buffer for 18 h at 4°C, blots were washed, incubated in HRP-conjugated secondary antibodies (1:2000 dilution; DAKO, Carpinteria, CA, USA), washed and the signals visualized using enhanced chemiluminescence reagents and film from GE Healthcare.

Confocal microscopy for colocalization

HEK293 cells were seeded on glass cover slips (9 × 9 mm, coated with 0.1% gelatin) and transiently co-transfected with pCMV-APP_{751}, WT CHIP and different cell compartment marker cDNAs (1 μg) described previously; 48 h after transfection, cells were fixed for 15 min at room temperature using 4% paraformaldehyde in PBS. After permeabilization and blocking, cells were incubated in primary antibody in PBS containing 0.4% BSA and 5% goat serum overnight at 4°C. After washing, samples were incubated with goat-derived

secondary antibodies (1:200) labeled with Cy2 or Cy3 (Jackson Immuno Research, West Grove, PA, USA). After washing, the coverslips were mounted in DAKO-Fluoromount. Samples were examined using a Nikon C1 laser scanning confocal microscopy system in multi-tracking mode to eliminate signal bleed-through. All images were collected with a constant pinhole diameter at 40× in order to maintain the depth of focus.

RNA isolation and RT–PCR

Total cellular RNA was isolated from cultured cells, using the RNeasy mini kit, following the manufacturer's instructions (QIAGEN, Valencia, CA, USA). RNA was eluted with diethylpyrocarbonate-treated water or TE. For the synthesis of cDNA, 1 μg of random hexanucleotides (GE Healthcare) were annealed to 1–3 μg RNA in a 20 μl reaction volume after heating for 5 min at 95°C. The samples were transferred to room temperature and 30 μl of first-strand reverse transcriptase buffer containing 10 mM DTT, 2.4 mM dNTPs and 40 U/reaction reverse transcriptase was added. The reactions were incubated for 1 h at 37°C, followed by 7 min at 95°C for denaturation of the DNA and enzyme. The samples were kept on ice or stored at −20°C. For the PCR reaction, 3 μl of single-stranded cDNA was amplified in a reaction containing 10 mM Tris–HCl, pH9.0, 1.5 mM $MgCl_2$, 50 mM KCl, 10 pmol/reaction reverse and forward primer, 0.2 mM dNTPs and 1 U/reaction *Taq* DNA polymerase in a final volume of 30 μl (cycle condition: 95°C-5 min× 1 cycle; 95°C-1 min, 55–65°C-1.5 min. and 72°C-1.5 min × 25 cycles; 72°C-7 min× 1 cycle).

MTT cell viability assay

To measure cell viability, cells were washed twice in warm D-PBS and incubated in 1 ml DMEM containing 0.5 mg MTT (Molecular Probes, Eugene, OR, USA) for 2–3 h at 37°C and 5% CO_2. The medium was aspirated and the cells were washed twice with PBS at room temperature. Formazan salt was dissolved in 1 ml pure ethanol. Cells were homogenized by repetitive pipetting, followed by centrifugation for 5 min at 4500 r.p.m. (1700*g*) and the supernatant collected by careful decanting to avoid re-dissolving the protein pellet in ethanol. The absorbance was read against an ethanol blank at 564 nm in a PerSeptive CytoFluor4000 (ABI).

Pulse-chase labeling studies

APP751-HEK stable cell line cultures in 35 mm dishes were starved for 30 min in DMEM without methionine and cysteine. The cultures were pulsed for 30 min in the same medium (500 μl) containing 100 μCi/ml of a ^{35}S-methionine/cysteine mixture (Expre^{35}SS labeling mix; Perkin-Elmer LifeSciences, Boston, MA, USA). Cultures were cold-chased using complete, serum-containing medium without radioactive amino acids for various times [up to 2 h (APP) and 6 h (Aβ)] after the pulse. Cells were harvested in Triton lysis buffer, as previously described (38). Full-length APP was immunoprecipitated using rabbit polyclonal anti-APP (C8), followed by 30 μl protein A/G Sepharose beads. After centrifugation at 14 000*g* for 5 min at 4°C and washing, proteins were eluted directly from the beads in SDS sample buffer with heating to 95°C for 10 min and then electrophoresed on 10% polyacrylamide Ready-Gels (Bio-Rad, Richmond, CA, USA). After electrophoresis, gels were treated for fluorography using EnHance (PE Life-Sciences, Boston, MA, USA), dried and exposed to Kodak X-OMat AR-5 film at −70°C.

Densitometry and statistical analysis

Multiple film exposures were obtained to assure that experimental images were within a linear, usable response range. Images were scanned and analyzed using QuantiScan densitometry software (BioSoft, Ferguson, MO, USA). Areas under the peak were determined. All experimental samples were corrected and normalized relative to an internal control (i.e. Cdk4 or actin). Data are expressed as mean ± SEM, and statistical evaluation was performed by using Student's *t*-test for paired or unpaired data and one-way ANOVA followed by Bonferroni's correction or ANOVA for repeated measures, where appropriate. Values of $P < 0.05$ were considered statistically significant.

ACKNOWLEDGEMENTS

This work was supported in part by a grant from the NINDS to H.W.Q. (NS 41371). We are grateful to Dr Dennis Selkoe for antibodies C8 and R1282 and for the HEK751 cell lines. The authors thank the Harvard Brain Tissue Resources Center, supported in part by PHS grant R24-MH068855, for rapid frozen adult human brain samples.

Conflict of Interest statement. There is no financial or other conflict of interest pertaining to any of the results or conclusion cited in this manuscript.

REFERENCES

1. LaFerla, F.M., Hall, C.K., Ngo, L. and Jay, G. (1996) Extracellular deposition of beta-amyloid upon p53-dependent neuronal cell death in transgenic mice. *J. Clin. Invest.*, **98**, 1626–1632.
2. Yang, Y., Turner, R.S. and Gaut, J.R. (1998) The chaperone BiP/GRP78 binds to amyloid precursor protein and decreases Abeta40 and Abeta42 secretion. *J. Biol. Chem.*, **273**, 25552–22555.
3. Patrick, G.N., Zukerberg, L., Nikolic, M., de la Monte, S., Dikkes, P. and Tsai, L.H. (1999) Conversion of p35 to p25 deregulates Cdk5 activity and promotes neurodegeneration. *Nature*, **402**, 615–622.
4. Gouras, G.K., Tsai, J., Naslund, J., Vincent, B., Edgar, M., Checler, F., Greenfield, J.P., Haroutunian, V., Buxbaum, J.D., Xu, H., Greengard, P. and Relkin, N.R. (2000) Intraneuronal Abeta42 accumulation in human brain. *Am. J. Pathol.*, **156**, 15–20.
5. Walsh, D.M., Tseng, B.P., Rydel, R.E., Podlisny, M.B. and Selkoe, D.J. (2000) The oligomerization of amyloid beta-protein begins intracellularly in cells derived from human brain. *Biochemistry*, **39**, 10831–10839.
6. D'Andrea, M.R., Nagele, R.G., Wang, H.Y., Peterson, P.A. and Lee, D.H. (2001) Evidence that neurones accumulating amyloid can undergo lysis to form amyloid plaques in Alzheimer's disease. *Histopathology*, **38**, 120–134.
7. Gyure, K.A., Durham, R., Stewart, W.F., Smialek, J.E. and Troncoso, J.C. (2001) Intraneuronal abeta-amyloid precedes development of amyloid plaques in Down syndrome. *Arch. Pathol. Lab. Med.*, **125**, 489–492.
8. Busciglio, J., Pelsman, A., Wong, C., Pigino, G., Yuan, M., Mori, H. and Yankner, B.A. (2002) Altered metabolism of the amyloid beta precursor protein is associated with mitochondrial dysfunction in Down's syndrome. *Neuron*, **33**, 677–688.
9. Takahashi, R.H., Nam, E.E., Edgar, M. and Gouras, G.K. (2002) Alzheimer beta-amyloid peptides: normal and abnormal localization. *Histol. Histopathol.*, **17**, 239–246.

10. Bonini, N.M. (2002) Chaperoning brain degeneration. *Proc. Natl Acad. Sci. USA*, **99** (Suppl. 4), 16407–16411.
11. Sakahira, H., Breuer, P., Hayer-Hartl, M.K. and Hartl, F.U. (2002) Molecular chaperones as modulators of polyglutamine protein aggregation and toxicity. *Proc. Natl Acad. Sci. USA*, **99** (Suppl. 4), 16412–16418.
12. Shimura, H., Schwartz, D., Gygi, S.P. and Kosik, K.S. (2004) CHIP-Hsc70 complex ubiquitinates phosphorylated tau and enhances cell survival. *J. Biol. Chem.*, **279**, 4869–4876.
13. Miller, V.M., Nelson, R.F., Gouvion, C.M., Williams, A., Rodriguez-Lebron, E., Harper, S.Q., Davidson, B.L., Rebagliati, M.R. and Paulson, H.L. (2005) CHIP suppresses polyglutamine aggregation and toxicity *in vitro* and *in vivo*. *J. Neurosci.*, **25**, 9152–9161.
14. Magrane, J., Smith, R.C., Walsh, K. and Querfurth, H.W. (2004) Heat shock protein 70 participates in the neuroprotective response to intracellularly expressed beta-amyloid in neurons. *J. Neurosci.*, **24**, 1700–1706.
15. Magrané, J., Rosen, K.M., Smith, R.C., Walsh, K., Gouras, G.K. and Querfurth, H.W. (2005) Intraneuronal β-amyloid expression down-regulates the Akt survival pathway and suppresses the stress response. *J. Neurosci.*, **25**, 10960–10969.
16. Ballinger, C.A., Connell, P., Wu, Y., Hu, Z., Thompson, L.J., Yin, L.Y. and Patterson, C. (1999) Identification of CHIP, a novel tetratricopeptide repeat-containing protein that interacts with heat shock proteins and negatively regulates chaperone functions. *Mol. Cell. Biol.*, **19**, 4535–4545.
17. Connell, P., Ballinger, C.A., Jiang, J., Wu, Y., Thompson, L.J., Hohfeld, J. and Patterson, C. (2001) The co-chaperone CHIP regulates protein triage decisions mediated by heat-shock proteins. *Nat. Cell Biol.*, **3**, 93–96.
18. Kampinga, H.H., Kanon, B., Salomons, F.A., Kabakov, A.E. and Patterson, C. (2003) Overexpression of the cochaperone CHIP enhances Hsp70-dependent folding activity in mammalian cells. *Mol. Cell. Biol.*, **23**, 4948–4958.
19. Dai, Q., Qian, S.B., Li, H.H., McDonough, H., Borchers, C., Huang, D., Takayama, S., Younger, J.M., Ren, H.Y., Cyr, D.M. and Patterson, C. (2005) Regulation of the cytoplasmic quality control protein degradation pathway by BAG2. *J. Biol. Chem.*, **280**, 38673–38681.
20. Hwang, J.R., Zhang, C. and Patterson, C. (2005) C-terminus of heat shock protein 70 interacting protein facilitates degradation of apoptosis signal-regulating kinase1 and inhibits apoptosis signal-regulating kinase-1 dependent apoptosis. *Cell Stress Chaperones*, **10**, 147–156.
21. Aravind, L. and Koonin, E.V. (2000) The U box is a modified RING finger—a common domain in ubiquitination. *Curr. Biol.*, **10**, R132–R134.
22. Wickner, S., Maurizi, M. and Gottesman, S. (1999) Posttranslational quality control: folding, refolding and degradation of proteins. *Science*, **286**, 1888–1893.
23. McClellan, A.J. and Frydman, J. (2001) Molecular chaperones and the art of recognizing a lost cause. *Nat. Cell Biol.*, **3**, E51–E53.
24. McDonough, H. and Patterson, C. (2003) CHIP: a link between the chaperone and proteasome systems. *Cell Stress Chaperones*, **8**, 303–308.
25. Jana, N.R., Dikshit, P., Goswami, A., Kotliarova, S., Murata, S., Tanaka, K. and Nukina, N. (2005) Co-chaperone CHIP associates with expanded polyglutamine proteins and promotes their degradation by proteasomes. *J. Biol. Chem.*, **280**, 11635–11640.
26. Imai, Y., Soda, M., Hatakeyama, S., Akagi, T., Hashikawa, T., Nakayama, K.I. and Takahashi, R. (2002) CHIP is associated with Parkin, a gene responsible for familial Parkinson's disease, and enhances its ubiquitin ligase activity. *Mol. Cell*, **10**, 55–67.
27. Shin, Y., Klucken, J., Patterson, C., Hyman, B.T. and McLean, P.J. (2005) The co-chaperone carboxyl terminus of Hsp70-interacting protein (CHIP) mediates alpha-synuclein degradation decisions between proteasomal and lysosomal pathways. *J. Biol. Chem.*, **280**, 23727–23734.
28. Meacham, G.C., Patterson, C., Zhang, W., Younger, J.M. and Cyr, D.M. (2001) The Hsc70 co-chaperone CHIP targets immature CFTR for proteasomal degradation. *Nat. Cell Biol.*, **3**, 100–105.
29. Younger, J.M., Ren, H.Y., Chen, L., Fan, C.Y., Fields, A., Patterson, C. and Cyr, D.M. (2004) A foldable CFTR {Delta} F508 biogenic intermediate accumulates upon inhibition of the Hsc70-CHIP E3 ubiquitin ligase. *J. Cell Biol.*, **167**, 1075–1085.
30. Hatakeyama, S., Matsumoto, M., Kamura, T., Murayama, M., Chui, D.H., Planel, E., Takahashi, R., Nakayama, K.I. and Takashima, A. (2004) U-box protein carboxyl terminus of Hsc70-interacting protein (CHIP) mediates poly-ubiquitylation preferentially on four-repeat tau and is involved in neurodegeneration of tauopathy. *J. Neurochem.*, **91**, 299–307.
31. Petrucelli, L., Dickson, D., Kehoe, K., Taylor, J., Snyder, H., Grover, A., De Lucia, M., McGowan, E., Lewis, J., Prihar, G. *et al*. (2004) CHIP and Hsp70 regulate tau ubiquitination, degradation and aggregation. *Hum. Mol. Genet.*, **13**, 703–714.
32. Sahara, N., Murayama, M., Mizoroki, T., Urushitani, M., Imai, Y., Takahashi, R., Murata, S., Tanaka, K. and Takashima, A. (2005) *In vivo* evidence of CHIP up-regulation attenuating tau aggregation. *J. Neurochem.*, **94**, 1254–1263.
33. Morimoto, R.I. (1998) Regulation of the heat shock transcriptional response: cross talk between a family of heat shock factors, molecular chaperones and negative regulators. *Genes Dev.*, **12**, 3788–3796.
34. Dai, Q., Zhang, C., Wu, Y., McDonough, H., Whaley, R.A., Godfrey, V., Li, H.H., Madamanchi, N., Xu, W., Neckers, L., Cyr, D. and Patterson, C. (2003) CHIP activates HSF1 and confers protection against apoptosis and cellular stress. *EMBO J.*, **22**, 5446–5458.
35. Qian, S.B., McDonough, H., Boellmann, F., Cyr, D.M. and Patterson, C. (2006) CHIP-mediated stress recovery by sequential ubiquitination of substrates and Hsp70. *Nature*, **440**, 551–555.
36. Nunan, J., Williamson, N.A., Hill, A.F., Sernee, M.F., Masters, C.L. and Small, D.H. (2003) Proteasome-mediated degradation of the C-terminus of the Alzheimer's disease beta-amyloid protein precursor: effect of C-terminal truncation on production of beta-amyloid protein. *J. Neurosci. Res.*, **74**, 378–385.
37. Nunan, J., Shearman, M.S., Checler, F., Cappai, R., Evin, G., Beyreuther, K., Masters, C.L. and Small, D.H. (2001) The C-terminal fragment of the Alzheimer's disease amyloid protein precursor is degraded by a proteasome-dependent mechanism distinct from gamma-secretase. *Eur. J. Biochem.*, **268**, 5329–5336.
38. Rosen, K.M., Ford, B.D. and Querfurth, H.W. (2003) Downregulation and increased turnover of beta-amyloid precursor protein in skeletal muscle cultures by neuregulin-1. *Exp. Neurol.*, **181**, 170–180.
39. Bush, K.T., Goldberg, A.L. and Nigam, S.K. (1997) Proteasome inhibition leads to a heat-shock response, induction of endoplasmic reticulum chaperones, and thermotolerance. *J. Biol. Chem.*, **272**, 9086–9092.
40. Veereshwarayya, V., Kumar, P., Rosen, K.M., Mestril, R. and Querfurth, H.W. (2006) Differential effects of mitochondrial Hsp60 and related molecular chaperones to prevent intracellular β-amyloid induced inhibition of complex IV and limit apoptosis. *J. Biol. Chem.*, **281**, 29468–29478.
41. Demand, J., Alberti, S., Patterson, C. and Hohfeld, J. (2001) Cooperation of a ubiquitin domain protein and an E3 ubiquitin ligase during chaperone/proteasome coupling. *Curr. Biol.*, **11**, 1569–1577.
42. Murata, S., Minami, Y., Minami, M., Chiba, T. and Tanaka, K. (2001) CHIP is a chaperone-dependent E3 ligase that ubiquitylates unfolded protein. *EMBO Rep.*, **2**, 1133–1138.
43. Murata, S., Chiba, T. and Tanaka, K. (2003) CHIP: a quality control E3 ligase collaborating with molecular chaperones. *Int. J. Biochem. Cell. Biol.*, **35**, 572–578.
44. Hatakeyama, S., Yada, M., Matsumoto, M., Ishida, N. and Nakayama, K.I. (2001) U box proteins as a new family of ubiquitin-protein ligases. *J. Biol. Chem.*, **276**, 33111–33120.
45. da Costa, C.A., Ancolio, K. and Checler, F. (1999) C-terminal maturation fragments of presenilin 1 and 2 control secretion of APP alpha and A beta by human cells and are degraded by proteasome. *Mol. Med.*, **5**, 160–168.
46. Marambaud, P., Lopez-Perez, E., Wilk, S. and Checler, F. (1997) Constitutive and protein kinase C-regulated secretory cleavage of Alzheimer's beta-amyloid precursor protein: different control of early and late events by the proteasome. *J. Neurochem.*, **69**, 2500–2505.
47. Golde, T.E., Estus, S., Younkin, L.H., Selkoe, D.J. and Younkin, S.G. (1992) Processing of the amyloid protein precursor to potentially amyloidogenic derivatives. *Science*, **255**, 728–730.
48. Knauer, M.F., Soreghan, B., Burdick, D., Kosmoski, J. and Glabe, C.G. (1992) Intracellular accumulation and resistance to degradation of the Alzheimer amyloid A4/beta protein. *Proc. Natl Acad. Sci. USA*, **89**, 7437–7441.
49. Munger, J.S., Haass, C., Lemere, C.A., Shi, G.P., Wong, W.S., Teplow, D.B., Selkoe, D.J. and Chapman, H.A. (1995) Lysosomal processing of amyloid precursor protein to A beta peptides: a distinct role for cathepsin S. *Biochem. J.*, **311**, 299–305.

50. Haass, C., Lemere, C.A., Capell, A., Citron, M., Seubert, P., Schenk, D., Lannfelt, L. and Selkoe, D.J. (1995) The Swedish mutation causes early-onset Alzheimer's disease by beta-secretase cleavage within the secretory pathway. *Nat. Med.*, **1**, 1291–1296.
51. Cupers, P., Orlans, I., Craessaerts, K., Annaert, W. and De Strooper, B. (2001) The amyloid precursor protein (APP)-cytoplasmic fragment generated by gamma-secretase is rapidly degraded but distributes partially in a nuclear fraction of neurones in culture. *J. Neurochem.*, **78**, 1168–1178.
52. Pasternak, S.H., Bagshaw, R.D., Guiral, M., Zhang, S., Ackerley, C.A., Pak, B.J., Callahan, J.W. and Mahuran, D.J. (2003) Presenilin-1, nicastrin, amyloid precursor protein, and gamma-secretase activity are co-localized in the lysosomal membrane. *J. Biol. Chem.*, **278**, 26687–26694.
53. Selkoe, D.J. and Schenk, D. (2003) Alzheimer's disease: molecular understanding predicts amyloid-based therapeutics. *Annu. Rev. Pharmacol. Toxicol.*, **43**, 545–584.
54. Schmitz, A., Schneider, A., Kummer, M.P. and Herzog, V. (2004) Endoplasmic reticulum-localized amyloid beta-peptide is degraded in the cytosol by two distinct degradation pathways. *Traffic*, **5**, 89–101.
55. Dickey, C.A., Yue, M., Lin, W.L., Dickson, D.W., Dunmore, J.H., Lee, W.C., Zehr, C., West, G., Cao, S., Clark, A.M.K. *et al*. (2006) Deletion of the ubiquitin ligase CHIP leads to the accumulation, but not the aggregation, of both endogenous phospho- and Caspase-3-cleaved tau species. *J. Neurosci.*, **26**, 6985–6996.
56. Imai, Y., Soda, M., Inoue, H., Hattori, N., Mizuno, Y. and Takahashi, R. (2001) An unfolded putative transmembrane polypeptide, which can lead to endoplasmic reticulum stress, is a substrate of Parkin. *Cell*, **105**, 891–902.
57. Zhou, P., Fernandes, N., Dodge, I.L., Reddi, A.L., Rao, N., Safran, H., DiPetrillo, T.A., Wazer, D.E., Band, V. and Band, H. (2003) ErbB2 degradation mediated by the co-chaperone protein CHIP. *J. Biol. Chem.*, **278**, 13829–13837.
58. Querfurth, H.W., Jiang, J., Geiger, J.D. and Selkoe, D.J. (1997) Caffeine stimulates amyloid beta-peptide release from beta-amyloid precursor protein-transfected HEK293 cells. *J. Neurochem.*, **69**, 1580–1591.
59. Coaxum, S.D., Martin, J.L. and Mestril, R. (2003) Overexpression of heat shock proteins differentially modulates protein kinase C expression in rat neonatal cardiomyocytes. *Cell Stress Chaperones.*, **8**, 297–302.